N-Me, a long range oncogenic enhancer in T-cell acute lymphoblastic leukemia

Daniel Herranz, Alberto Ambesi-Impiombato, Teresa Palomero, Stephanie A. Schnell, Laura Belver, Agnieszka A. Wendorff, Luyao Xu, Mireia Castillo, David Llobet-Navás, Carlos Cordon Cardo, Emmanuelle Clappier, Jean Soulier and Adolfo A. Ferrando

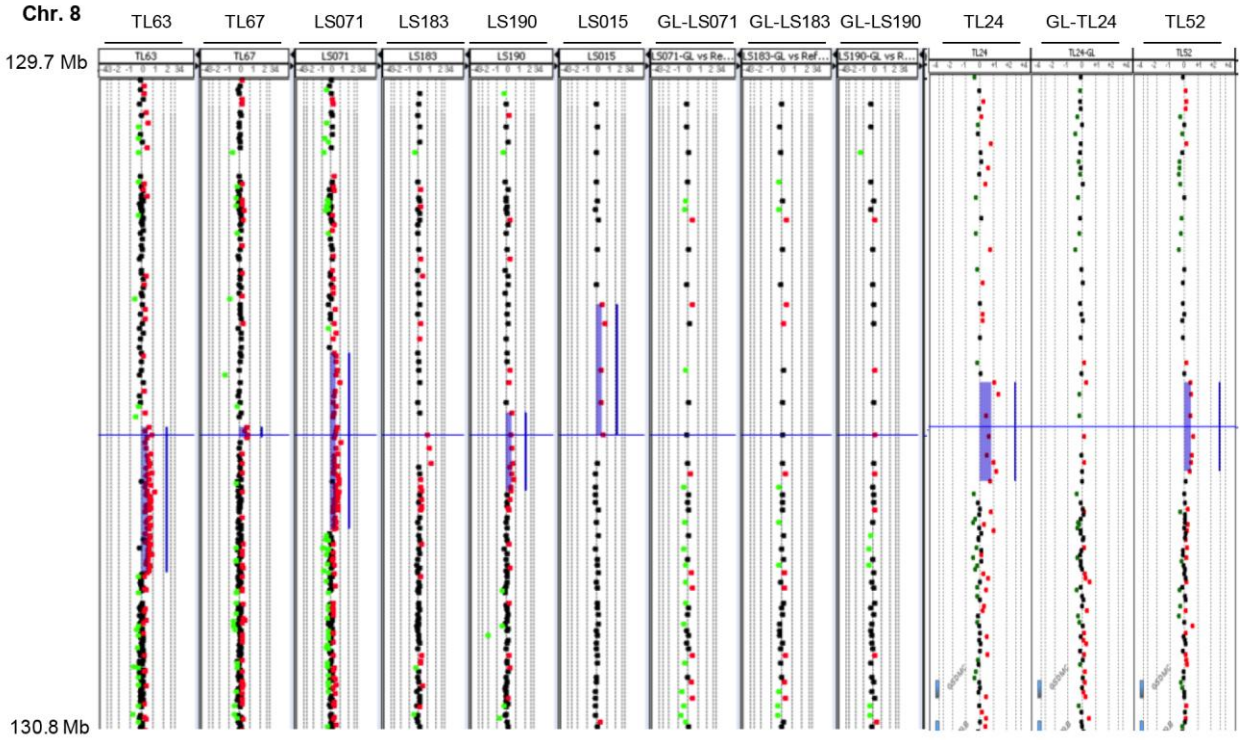

Supplementary Figure 1. Focal 8q24 duplications in T-ALL. plots showing recurrent duplications. Log2 ratio signal of tumor DNA compared to a normal reference control for array comparative genomic hybridization probes at 8q24 in primary T-ALL samples is shown. Paired germ-line samples (GL) are shown when available. Genomic areas indicated by the blue bars correspond to high confidence duplications as predicted by the ADM-2 tool (Agilent Technologies).

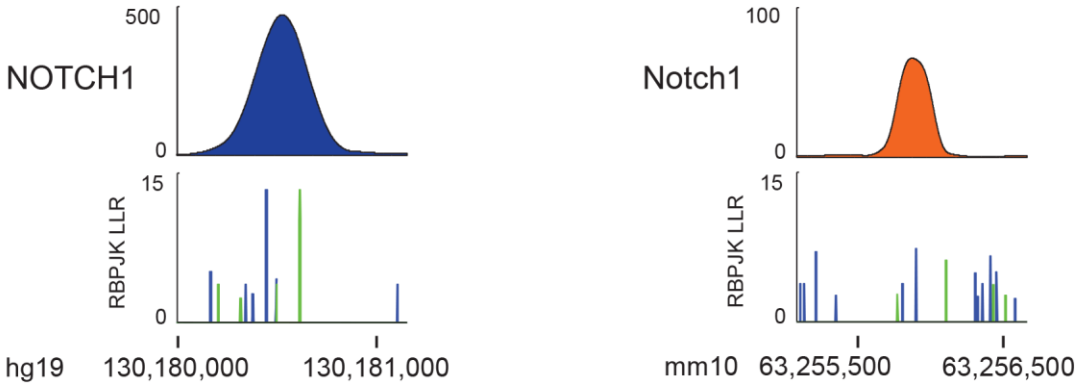

Supplementary Figure 2. Location of RBPJ binding sites within the NOTCH1 human and mouse N-Me enhancer sites. Top panels represent density of NOTCH1 ChIP-seq reads. Bottom panels indicate distribution of RBPJ matching sites (RBPJK LLR), with forward orientation sites shown as blue bars and reverse orientation sites shown as green bars. Y axis indicates likelihood of RBPJ matching (fold over random).

a

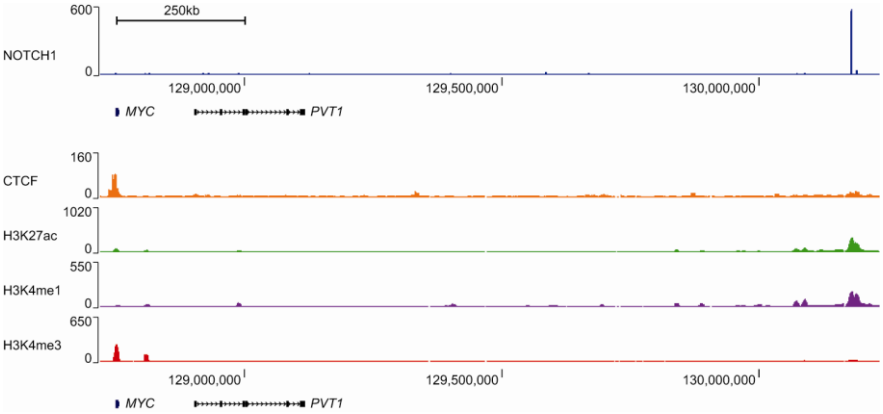

b

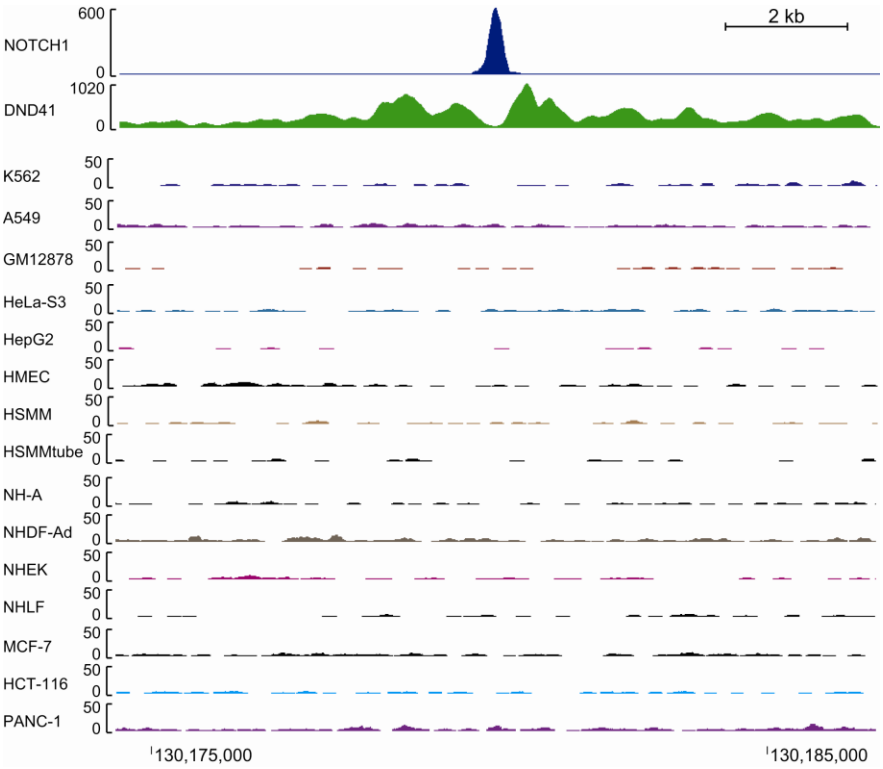

Supplementary Figure 3. Chromatin marks along windows containing the *MYC* +1.47 Mb NOTCH1 binding site (**a**) NOTCH1, CTCF, H3K27ac, H3K4me1 and H3K4me3 ChIP-seq occupancy along a 1.5 Mb window. NOTCH1 track represents ChIP-seq data from HPB-ALL cells. CTCF, H3K27ac, H3K4me1 and H3K4me3 tracks show ENCODE data in the DND41 T-ALL cell line. (**b**) H3K27ac ChIP-seq occupancy along a 10 Kb window in DND41 T-ALL cells and non T-ALL cell lines.

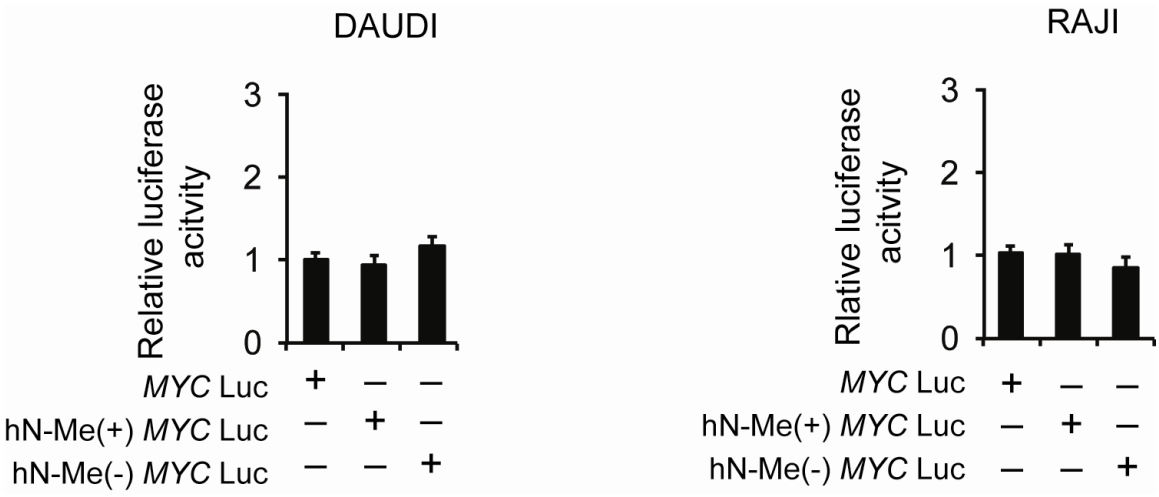

Supplementary Figure 4. Luciferase reporter activity in 293T cells transfected with of a *MYC* promoter construct (*MYC* Luc), a *MYC* promoter plus human N-Me enhancer in + orientation (hN-Me(+) *MYC* Luc), and a *MYC* promoter plus human N-Me enhancer in – orientation (hN-Me(–) *MYC* Luc) in DAUDI and RAJI B-cells.

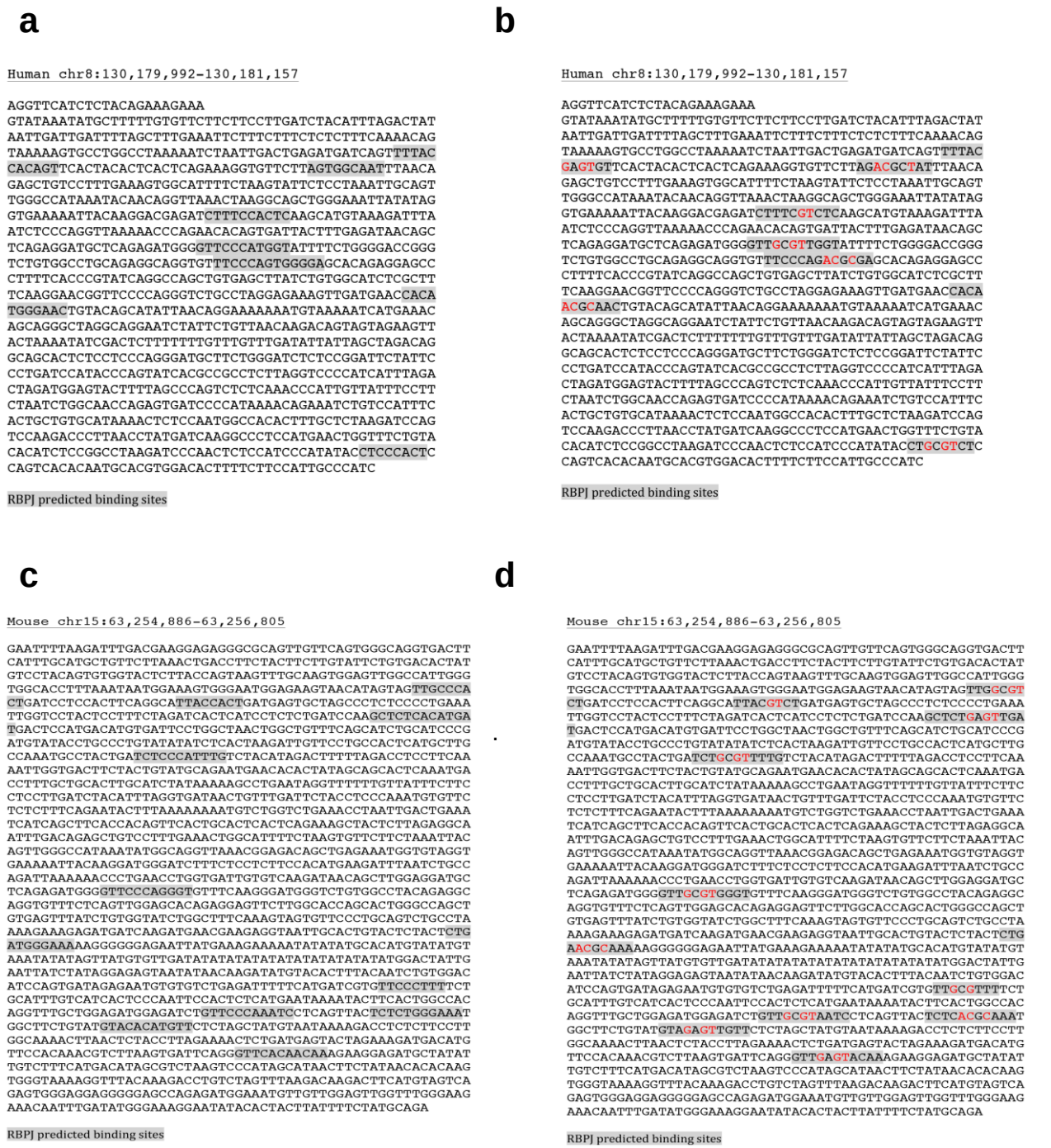

Supplementary Figure 5. N-Me DNA sequence. (**a**) Human N-Me wild type sequence. (**b**) Human N-Me sequence containing mutations in 7 RBPJ binding sites. Mutated bases are shown in red. (**c**) Mouse N-Me wild type sequence. (**d**) Mouse N-Me sequence containing mutations in 11 RBPJ binding sites. Mutated bases are shown in red

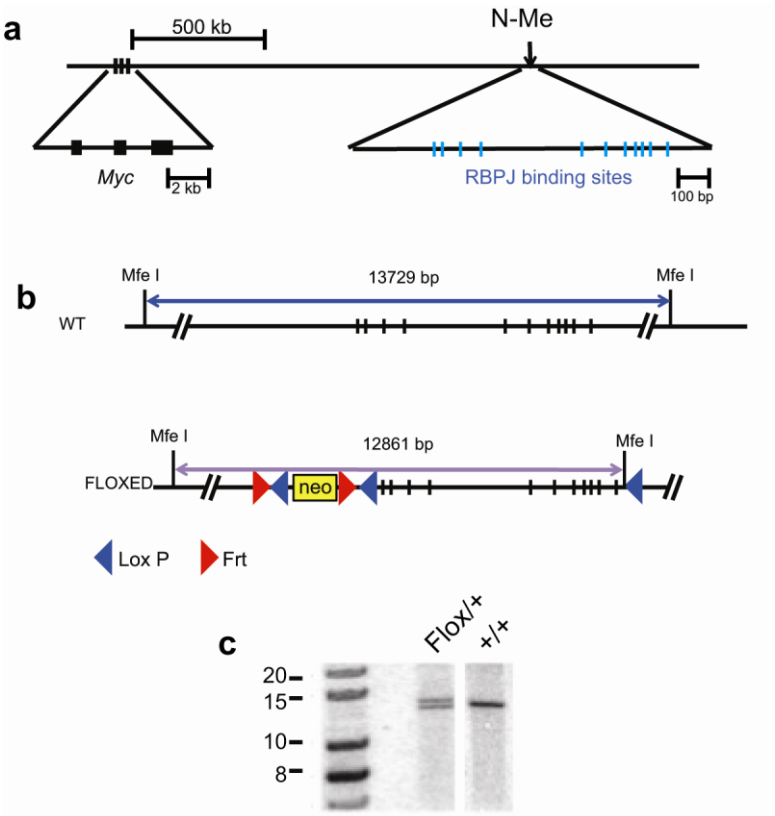

Supplementary Figure 6. Conditional targeting of the N-Me enhancer in mouse embryonic stem cells. (**a**) Schematic representation of the mouse *Myc* locus indicating the position of the N-Me enhancer. (**b**) Schematic representation of the targeting strategy for generation of N-Me conditional knockout allele. (**c**) Southern blot analysis of N-Me targeted embryonic stem cells in DNA digestions with the *Mfe*I restriction enzyme hybridized with a long arm DNA probe. (**d**) Schematic representation of the breeding strategy for the generation of N-Me knockout and conditional knockout mice.

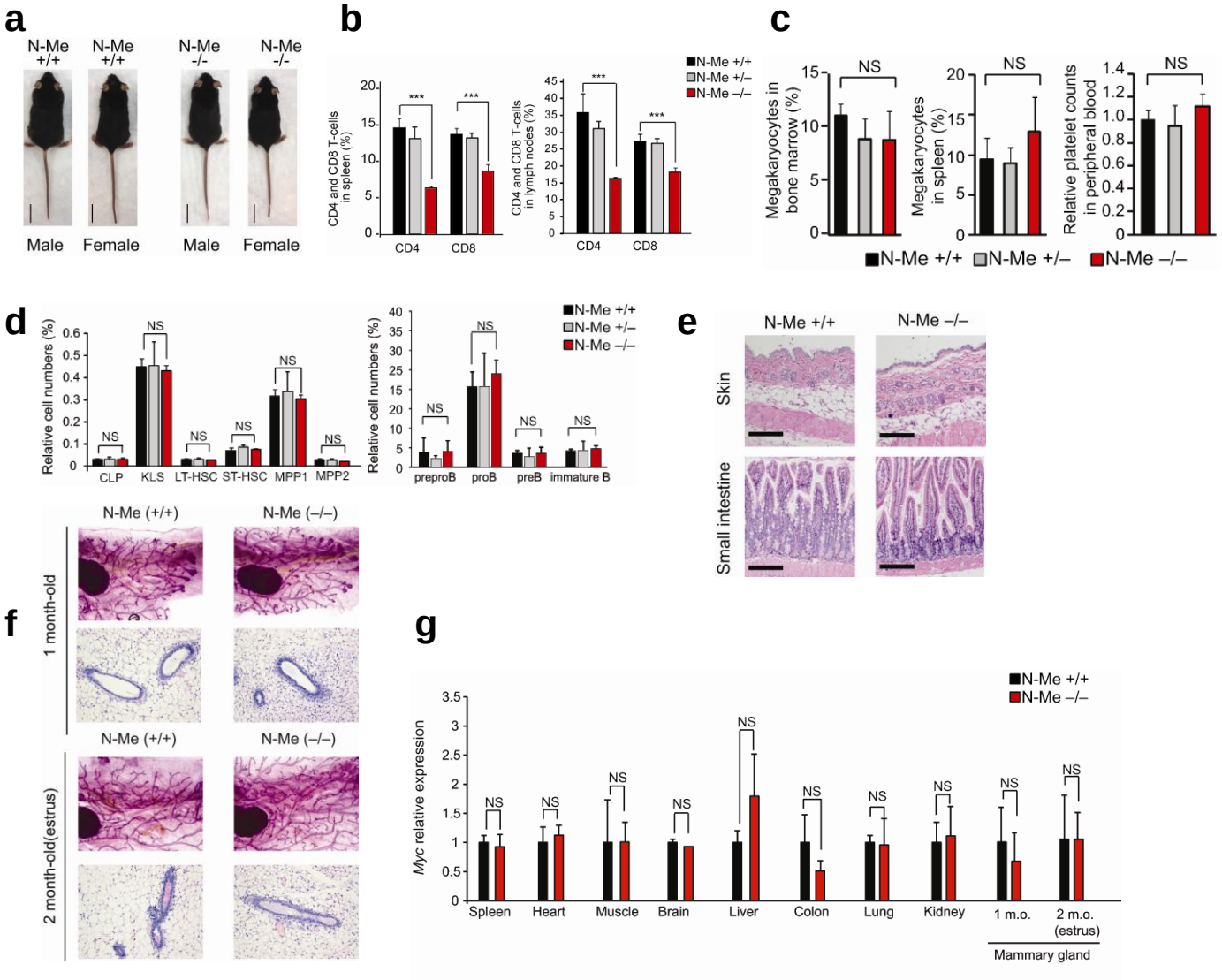

Supplementary Figure 7. Phenotypic characterization of N-Me knockout mice. (**a**) Representative images of 6 week-old N-Me conditional knockout mice and littermate wild type controls. Scale bar: 2 cm. (**b**) Quantification of T-cell populations in spleen and lymph nodes of N-Me wild type, heterozygous or homozygous knockout mice. (**c**) Quantification of megakaryocytes in bone marrow and spleen and platelets in peripheral blood from N-Me wild type, heterozygous or homozygous knockout mice. (**d**) Quantification of bone marrow stem cells, lymphoid and myeloid progenitors in N-Me wild type, N-Me heterozygous and N-Me null mice. CLP: common lymphocyte progenitors. KLS: cKit+, Lin-, Sca1+ population. LT-HSC: long term hematopoietic stem cells. ST-HSC: short term hematopoietic stem cells. MPP1: multipotential progenitor 1 population. MPP2: multipotential progenitor 2 population. Bar graphs indicate mean values and error bars represent s.d. (**e**) Hematoxylin eosin stained microphotographs of skin and small intestine from wild type and N-Me knockout mice. Scale bar: 100 µm (**f**) Carmine red stained and hematoxylin/eosin stained microphotographs of mammary glands from wild type and N-Me knockout females. Scale bar: 100µm. (**g**) RT-PCR analysis of *Myc* expression in tissues from wild type and N-Me knockout mice. Bar graphs indicate mean values and error bars represent s.d. *P* values in (**b,c,d,g**) were calculated using the two-tailed Student's *t*-test: NS= not significant; ****P*≤0.005.

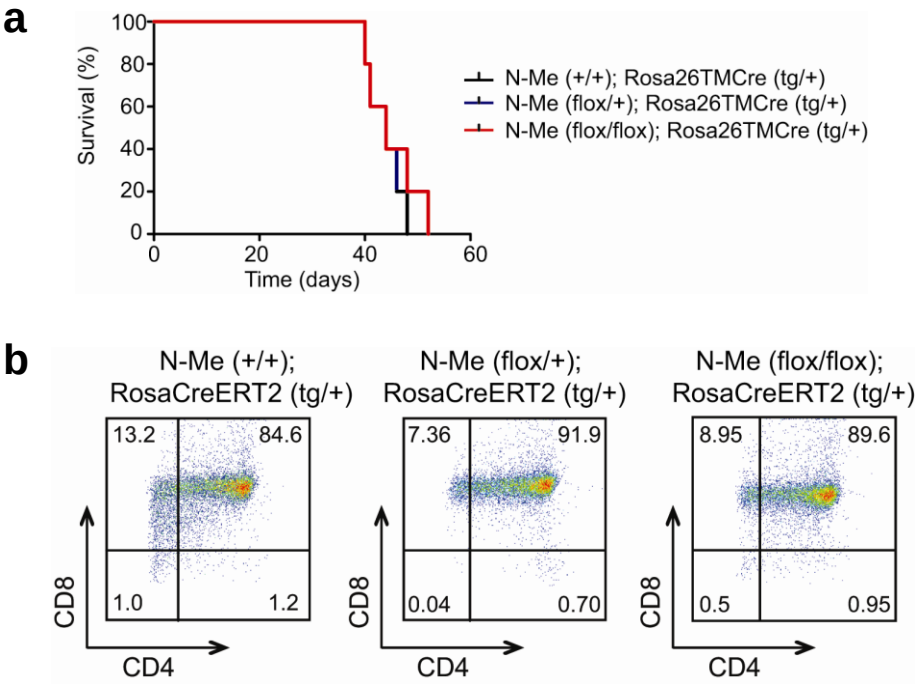

Supplementary Figure 8. Generation of wild type and inducible conditional N-Me heterozygous and homozygous knockout NOTCH1 induced T-ALLs. (**a**) Kaplan-Meier survival curves of mice transplanted with wild type and conditional N-Me heterozygous and homozygous knockout hematopoietic progenitors infected with retroviruses driving expression of constitutively active ΔE-NOTCH1. (**b**). Representative FACs plots showing robust expression of CD4 and CD8 T-cell markers in wild type and inducible conditional N-Me heterozygous and homozygous knockout NOTCH1 induced T-ALLs.

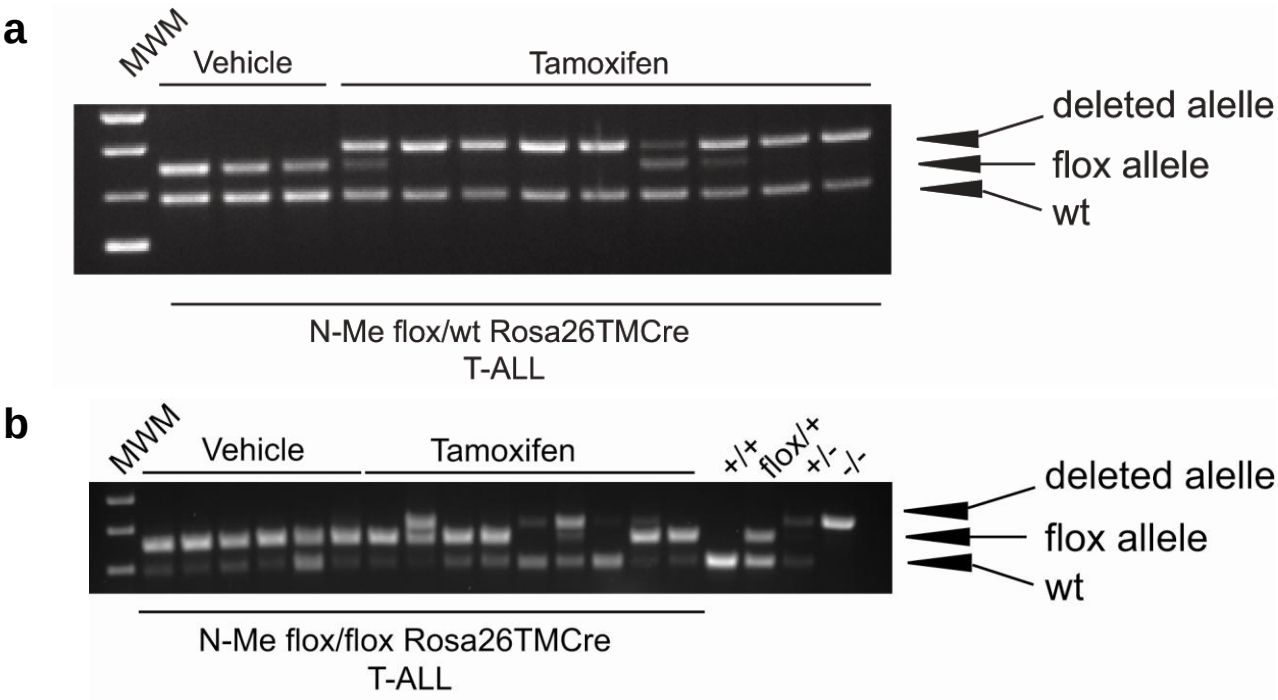

Supplementary Figure 9. PCR analysis of N-Me loss in NOTCH1-induced tumors with secondary (tamoxifen-induced) deletion of N-Me at the time of tumor progression. (**a**) DNA from N-Me conditional heterozygous NOTCH1 induced leukemias treated with vehicle only, or with tamoxifen to induce the deletion of one copy of N-Me, was recovered from the spleen of moribund mice at the time of overt tumor progression and was analyzed by PCR. (**b**) DNA from N-Me conditional homozygous knockout NOTCH1 induced leukemias treated with vehicle only, or with tamoxifen to induce the deletion of the 2 copies of N-Me, was recovered from the spleen of moribund mice at the time of overt tumor progression and was analyzed by PCR together with wild type, conditional heterozygous, deleted heterozygous and deleted homozygous controls. Wild type band in tumor samples is derived from residual recipient derived stroma cells.

a

N-Me (flox/flox); RosaTMCre (tg/+) – Vehicle treated		
Number of cells injected/mouse	Number of mice injected	Number of leukemia-developing mice
100.000	6	6
10.000	11	11
1.000	12	12
100	6	4
10	6	1
N-Me (flox/flox); RosaTMCre (tg/+) – Tamoxifen treated		
Number of cells injected/mouse	Number of mice injected	Number of leukemia-developing mice
100.000	6	6
10.000	12	5
1.000	10	2
100	6	0
10	6	0

b

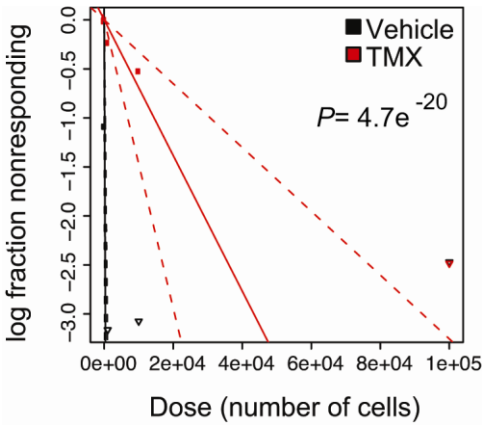

c

Confidence intervals for 1/(stem cell frequency)			
Group	Lower	Estimate	Upper
Vehicle	212	83.6	33.2
Tamoxifen	30728	14457	6802

Supplementary Figure 10. Effects of N-Me deletion in leukemia initiating cell activity. (**a**) Tumor incidence in mice treated with vehicle only (control) or tamoxifen (N-Me deletion) after transplantation of with serial dilutions of N-Me conditional knockout cells. (**b**) Serial dilution leukemia initiating cell analysis plot in mice treated with vehicle only (control) or tamoxifen (TMX, N-Me deletion) after transplantation of with serial dilutions of N-Me conditional knockout cells. (**c**) Confidence intervals showing 1/stem cell frequency.

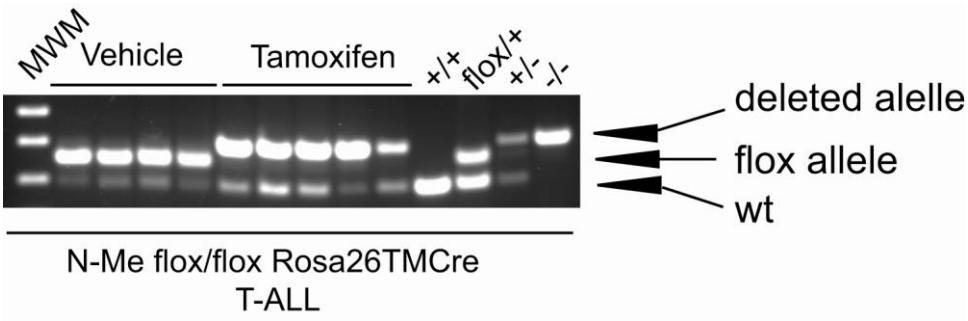

Supplementary Figure 11. PCR analysis of N-Me loss in NOTCH1-induced tumors after acute secondary (tamoxifen-induced) homozygous deletion of N-Me. DNA from N-Me conditional NOTCH1 induced leukemias treated with vehicle only or tamoxifen recovered from the spleen of mice 40 hours after treatment was analyzed by PCR together with wild type, conditional heterozygous, deleted heterozygous and deleted homozygous controls. Wild type band in tumor samples is derived from residual recipient derived stroma cells.

Supplementary Table 1. Recurrent focal genomic amplifications at +1.4 Mb downstream of *MYC* in T-ALL cases. Genomic positions in hg19 assembly are shown.

Case ID	CGH-array platform	Duplication Start (bp)	Duplication End (bp)	Duplication size (bp)
TL24	244K	130 041 807	130 324 436	282 629
TL52	244K	130 041 807	130 293 604	251 797
TL63	1000K	130 161 775	130 404 122	242 347
TL67	1000K	130 161 775	130 202 012	40 237
LS015	180K	129 957 380	130 233 454	276 074
LS071	1000K	130 055 124	130 342 220	287 096
LS183	400K	130 156 555	130 239 307	82 752
LS190	400K	130 140 325	130 282 315	141 990

Supplementary Table 2. Oncogenic annotations of the T-ALL cases with N-Me focal amplifications

Case ID	Oncogenic subtype	*NOTCH1* mutations	*FBXW7* mutations
TL24	TAL-R	p.L1600P, p.P2514fs	Neg
TL52	TLX1	p.L1585P	Neg
TL63	TLX3	p.L1574P, p.Q2519 fs	Neg
TL67	TLX3	p.L1585P	Neg
LS015	TLX1	p.F1590delinsW	Neg
LS071	CALM-AF10	na	na
LS183	TCRB-MYB	Neg	Neg
LS190	Unknown	Neg	Neg

TAL-R, TAL-related; Neg, negative; na, not available.

Supplementary Table 3. Genetic frequencies in N-Me flox/+ x N-Me flox/+ offspring and N-Me +/- x N-Me +/- offspring

N-Me flox/+ x N-Me flox/+		
Genotype	Expected Mendelian genetic frequencies (%)	Observed frequencies (%) (n=44)
N-Me +/+	25	25
N-Me +/-	50	45.5
N-Me -/-	25	29.5
N-Me +/- x N-Me +/-		
Genotype	Expected Mendelian genetic frequencies (%)	Observed frequencies (%) (n=38)
N-Me +/+	25	23.7
N-Me +/-	50	55.2
N-Me -/-	25	21

Supplementary Table 4. DAVID functional annotation analysis of downregulated genes upon N-Me deletion in NOTCH1 induced T-ALL cells

Term	Count	P Value	FDR
acetylation	56	3.64E-11	4.65E-08
GO:0005730~nucleolus	19	7.40E-11	9.23E-08
GO:0031974~membrane-enclosed lumen	34	1.57E-10	1.96E-07
GO:0070013~intracellular organelle lumen	33	2.92E-10	3.64E-07
GO:0043233~organelle lumen	33	3.12E-10	3.89E-07
GO:0034660~ncRNA metabolic process	16	6.15E-10	9.52E-07
GO:0034470~ncRNA processing	14	2.62E-09	4.06E-06
GO:0031981~nuclear lumen	27	9.12E-09	1.14E-05
GO:0005739~mitochondrion	30	6.66E-07	8.31E-04
GO:0042254~ribosome biogenesis	10	1.00E-06	1.55E-03
GO:0006399~tRNA metabolic process	10	1.08E-06	1.67E-03
GO:0003723~RNA binding	21	3.35E-06	4.48E-03
GO:0008033~tRNA processing	8	3.88E-06	6.01E-03
GO:0022613~ribonucleoprotein complex biogenesis	10	5.36E-06	8.30E-03
GO:0006396~RNA processing	16	1.38E-05	2.14E-02
trna processing	7	2.86E-05	3.66E-02
GO:0043232~intracellular non-membrane-bounded organelle	33	5.32E-05	6.64E-02
GO:0043228~non-membrane-bounded organelle	33	5.32E-05	6.64E-02
GO:0006364~rRNA processing	7	6.52E-05	1.01E-01
GO:0016072~rRNA metabolic process	7	7.04E-05	1.09E-01
transit peptide	15	1.17E-04	1.50E-01
GO:0044271~nitrogen compound biosynthetic process	12	1.23E-04	1.90E-01
nucleus	56	4.41E-04	5.63E-01
rna-binding	14	7.32E-04	9.33E-01
GO:0008652~cellular amino acid biosynthetic process	5	7.40E-04	1.14E+00
transit peptide:Mitochondrion	14	8.65E-04	1.25E+00
Isomerase	7	9.05E-04	1.15E+00
amino-acid biosynthesis	4	9.78E-04	1.24E+00
mitochondrion	18	1.37E-03	1.73E+00
GO:0006563~L-serine metabolic process	3	1.77E-03	2.70E+00
active site:Nucleophile	8	1.91E-03	2.75E+00
GO:0046394~carboxylic acid biosynthetic process	7	2.08E-03	3.17E+00

GO:0016053~organic acid biosynthetic process	7	2.08E-03	3.17E+00
methyltransferase	7	2.33E-03	2.94E+00
phosphoprotein	79	2.34E-03	2.96E+00
region of interest:S-adenosyl-L-methionine binding	4	3.01E-03	4.29E+00
purine biosynthesis	3	4.63E-03	5.77E+00
GO:0009309~amine biosynthetic process	5	4.82E-03	7.20E+00
GO:0009982~pseudouridine synthase activity	3	5.28E-03	6.83E+00
GO:0006974~response to DNA damage stimulus	9	5.52E-03	8.21E+00
GO:0006259~DNA metabolic process	11	6.11E-03	9.05E+00
GO:0009127~purine nucleoside monophosphate biosynthetic process	3	6.32E-03	9.34E+00
GO:0009168~purine ribonucleoside monophosphate biosynthetic process	3	6.32E-03	9.34E+00
GO:0001522~pseudouridine synthesis	3	6.32E-03	9.34E+00
GO:0009451~RNA modification	4	7.02E-03	1.03E+01
GO:0009064~glutamine family amino acid metabolic process	4	7.49E-03	1.10E+01
GO:0009167~purine ribonucleoside monophosphate metabolic process	3	8.40E-03	1.22E+01
GO:0009126~purine nucleoside monophosphate metabolic process	3	8.40E-03	1.22E+01